

Evaluating the Woody Species Diversity by Means of Remotely Sensed Spectral and Texture Measures in the Urban Forests

Ulas Yunus Ozkan¹ · Ibrahim Ozdemir² · Serhun Saglam¹ · Ahmet Yesil¹ · Tufan Demirel¹

Received: 27 March 2015 / Accepted: 5 January 2016 / Published online: 16 February 2016
© Indian Society of Remote Sensing 2016

Abstract There is an urgent need to obtain an accurate data on biological diversity and its temporal variation, in order to adopt an appropriate protection strategy to manage the urban forest remnants on sustainable manner for future generations. RapidEye Satellite images with spatial resolution of 5×5 m (orthorectified pixel size), ASTER VNIR images with spatial resolution of 15×15 m and Landsat-8 OLI images with spatial resolution of 30×30 m were used to evaluate the woody species diversity in urban forest remnants. Pearson Correlation Coefficient (PCC) was used to determine the relationships between the woody species diversity at Alpha (α) level and the spectral & texture properties derived from the satellite images. PCC test showed a positive significant relationship between the brightness of the RapidEye satellite image (i.e., Atmospherically Resistant Vegetation Index; ARVI) and the *Simpson's Diversity Index* (S) ($r = 0.80$, $p < 0.01$). In order to also estimate the beta (β) diversity in the study, the relationship between species rarefaction curves and spectral rarefaction curves was calculated through multiple regression analysis i.e., Landsat NDVI, ASTER NDVI and RapidEye NDVI (respectively, $R^2 = 0.99$; 0.99 ; 0.98 , $p < 0.01$). The findings of the study revealed that satellite image with a resolution of 5 m would be more appropriate to estimate the woody species diversity of urban forest remnants. However, medium resolution satellite images (Landsat) may be used to

examine the species rarefaction curve and β diversity in forest remnants.

Keywords Urban forest remnants · Satellite images · Woody species diversity · Rarefaction curves

Introduction

Urban forest remnants are an isolated patches of woody/tree vegetation which grows within city or town such as parks, wooded buffers, greenways etc. (Forman 2014). These remnants had formed due to the destruction of forests as a result of intensive urbanization. These areas may vary in shape, size and vegetation species diversity (McKinney 2002; Petr et al. 2004) and provide several goods (bye products) and services to the society (Asan et al. 2007; Sander et al. 2010). Now a day, protection of biological diversity, recreation and esthetic services are more important in urban forest remnants (Tyrväinen et al. 2005; Kark and Dearborn 2009). The urban forests have a rich diversity of plant species since they are not managed (Bagnall 1979; McKinney 2002; Petr et al. 2004). Furthermore, they contribute to the protection of the biological diversity by accommodating food, shelter, concealment and nest for a great number of animal species (Mansfield et al. 2005; Tyrväinen et al. 2005). Urban forest remnants are significant spaces where people learn about the nature within the heart of cities. People may enjoy aesthetic beauty, an ideal place for recreation, exercising, and trekking at the free of cost and due to easy access (Konijnendijk 2005; Tyrväinen et al. 2005; Kong et al. 2007).

Even though urban forest remnants are highly important, but unfortunately facing various threats such as air pollution, intensive utilization, excessive use of recreational activities, and illegal logging. These factors directly or indirectly altered

✉ Ulas Yunus Ozkan
uozkan@istanbul.edu.tr

¹ Faculty of Forestry, Department of Forest Management, Istanbul University, 34473 İstanbul, Turkey

² Faculty of Forestry, Wildlife Ecology and Management, Suleyman Demirel University, 32260 Cunur, Isparta, Turkey

the vegetation structure and species composition and also productivity. Therefore, efforts in recent years are increasing to protect the biological diversity in urban forest remnants (Alvey 2006; Kark and Dearborn 2009). It is very challenging to make such an evaluation by taking account of all components of biological diversity. Species diversity is the main component in the evaluation of biological diversity (Rocchini et al. 2004). The most accurate way of collecting the data needed to evaluate the biological diversity is taking the inventory based on intensive terrestrial measures. However, this is a labor-intensive process, expensive and time consuming (Gillespie et al. 2008; Mutowo and Murwira 2012). In practice, the inventory can be taken only for a small portion of the planning area due to the lack of resources and time (Luoto et al. 2002). Therefore, it is critically important to evaluate rapidly and monitor the spatial distribution and temporal variation in biological diversity in order to decide on the appropriate protection strategies (Nagendra 2001; Moser et al. 2002; Singh et al. 2010; Varghese, et al. 2010).

Satellite images have a great potential as a source of information to monitor the biological diversity at local, regional and national scales at species level (Luoto et al. 2002; Rocchini et al. 2007; Gillespie et al. 2008; Singh et al. 2010; Adam et al. 2012). There have been efforts to determine the species diversity through remotely sensed data (Bawa et al. 2002; Fairbank and McGwire 2004; Rocchini et al. 2004; Cayuela et al. 2006; Rocchini 2007; Levin et al. 2007; Oldeland et al. 2010). These studies usually focused on the relationships between the spectral values and the species diversity in the plots (α diversity). Besides, the species rarefaction function relying on dissimilarities in species between the plots (β diversity) was adapted by some researchers to the spectral rarefaction function relying on spectral difference (Rocchini et al. 2005; Rocchini et al. 2007; Rocchini et al. 2009; Rocchini et al. 2011). These studies explored the ways of estimating β diversity with the help of the spectral rarefaction curve derived from the presence/absence matrix created based on presence/absence of each Digital Numbers (DNs) in the plots. They were conducted mainly in natural forests, whereas they did not explore adequately the possibility of using satellite images to evaluate the species diversity in the urban forest remnants.

In recent years, there has been a great interest in the texture properties of the image (spatial orders of pixels) for natural resource applications of image analysis (Ozdemir et al. 2008; Kim et al. 2011; Ozdemir and Karnieli, 2011; Ardila et al. 2012; Ozdemir and Donoghue 2013; Dian et al. 2015). These studies reported that there are relations between textural properties and structural heterogeneity of the forest. However, the relationship between the species diversity and the texture properties of images has not been evaluated extensively yet. In studies related to species diversity, the alignment between the size of the object and the spatial resolution of the satellite

image is very important. The use of a satellite image with a coarser resolution compared to the size of the object may conceal the actual spatial heterogeneity and lead to the underestimation of species diversity (Rocchini et al. 2011). Mixed pixels constitute the most important problem encountered in using the satellite images for urban forest remnants as they contain rich species diversity (Hung 2002). For that reason, it is important to compare the satellite images of different spatial resolution in order to decide on the optimal spatial resolution in evaluating the species diversity in urban forest remnants.

This study aimed at exploring the possibilities to evaluate the woody species diversity in urban forest remnants by using satellite images of different spatial resolution. To this end, the relationships between the α diversity calculated by using terrestrial measures and observations and the spectral & texture properties measured on satellite images were evaluated. Then, it was tested whether or not β diversity can be estimated in urban forest remnants by using spectral rarefaction function.

Materials and Methods

Study Area

The study area covers the urban forest remnants in Istanbul that has the most crowded city in Turkey with a population of around 15 million people. The urban forest remnants both in the European side and the Asian side of Istanbul are located at altitudes starting from sea level up to 250 m (Fig. 1). Formerly being natural forests, these forest remnants have been preserved and survived until today while the species diversity has been enriched through planting of new plant species (Asan et al. 2007). Residents of Istanbul use these areas for recreation, sports, and education purpose.

Field Data

The study site was divided into square grids of 90×90 m. The focus of the study was comprised of the woody species diversity. Therefore, 35 square grids that did not contain man-made objects were selected as sampling units. Since, the urban forest remnants were rich in woody species diversity, the sampling units were further divided into sub-plots. The circular plots of a fixed size (400 m^2) were positioned on four corners and one in the center of the sampling units. In this way, the sampling pattern consisted of 35 sampling units and 175 sub-plots. The center of the plots was founded on the land with the help of GPS and applied to the land with a laser. The woody species diversity in the plots of 400 m^2 and the number of species were recorded in the inventory. The field study was performed between August 2014 and November 2014.

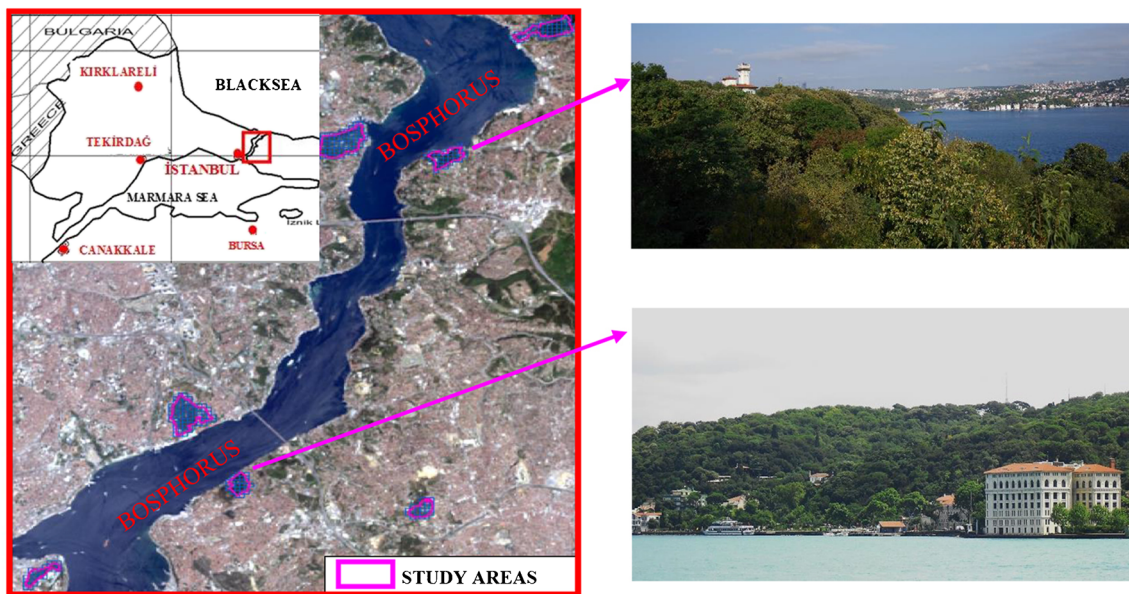


Fig. 1 Geographical location of the study site

Satellite Data

A RapidEye image with 6.5 m spatial resolution (5 m orthorectified pixel size), ASTER image with 15 m spatial resolution and Landsat-8 OLI image with 30 m spatial resolution were used in the study. The radiometric resolution of the RapidEye image is 12 bits and has 5 bands (Blue 440–510 nm; Green 520–590 nm; Red 630–685 nm; Red Edge 690–730 nm; Near Infrared 760–850 nm). ASTER image has a radiometric resolution of 8 bits and 3 bands in the Visible, Near Infrared (VNIR) (Green 0.52–0.60 μm , Red 0.63–0.69 μm , Near Infrared 0.76–0.86 μm). The Landsat 8 image that acquires images in the range of visible, near infrared, short wave infrared and thermal infrared has 5 bands in the Visible, Near Infrared (Coastal 0.433–0.453 μm , Blue 0.450–0.515 μm , Green 0.525–0.600 μm , Red 0.630–0.680, Near Infrared 0.845–0.885 μm). It has 12 bits radiometric resolution. RapidEye and ASTER images were obtained on 02 July 2014, while Landsat-8 image was obtained 30 June 2013.

In order to provide more detailed data regarding the areas that were covered with vegetation in multi-channel images, vegetation indexes were developed by using the original bands (Jensen and Lulla 1996). Four vegetation indexes (Atmospherically Resistant Vegetation Index-ARVI; Difference Vegetation Index-DVI; Infrared Percentage Vegetation Index-IPVI; Normalized Difference Vegetation Index-NDVI) were produced in the study in order to evaluate their potential for the evaluation of woody species diversity (Table 1).

Calculation of Spectral & Textural Properties

In the study, the texture properties were determined in addition to the spectral properties by using satellite images (Table 2).

The *Brightness* of the pixels in each image window corresponding to the sampling units were taken into account as the spectral properties. Texture properties were calculated according to *Grey Level Co-occurrence Matrix (GLCM)*. A large number of texture properties can be determined through *GLCM*. They are categorized under three main groups (Haralick et al. 1973). Those texture properties that are in the same group have high correlation with one another; therefore, one property from each group may suffice. Accordingly; “*Contrast*” from the contrast group; “*Entropy*” from the regularity group, and “*Correlation*” from the statistics group were used in the study. Spectral & texture properties were identified separately for the original bands of the satellite images or each set of data based on the original bands.

Alpha (α) Diversity

In the study, α diversity was represented by *Species Richness*, *Shannon-Wiener Diversity Index* (Shannon and Weaver 1949), *Simpson’s* (Simpson 1949) *Diversity Index* and *Species Mingling Index* (Gadow and Hui 2002) (Table 3). *Species Richness* refers to the total number of the sampled species in the area and it is acknowledged as the simplest indicator of biological diversity (Battles et al. 2001; Rocchini et al. 2005). *Shannon-Wiener Index* combines both number of species and their evenness into a single measure. *Simpson’s Index* is a dominance index that differently assigns weight to common or dominant species. The main principle of the *Species Mingling Index* is based on the neighborhood of the four closest trees to the reference tree.

For each sampling unit, the correlation analysis was applied to test whether, there is a significant association between the α diversity or not by taking the average of the species

Table 1 Vegetation indexes obtained from the satellite images

RapidEye	ASTER	Landsat-8 ETM	Equation	Author
ARVI		ARVI	$\frac{NIR-rb}{NIR+rb}$	Kaufman and Tanre 1992
DVI	DVI	DVI	NIR - RED	Tucker 1979
IPVI	IPVI	IPVI	$\frac{NIR}{NIR+RED}$	Crippen 1990
NDVI	NDVI	NDVI	$\frac{NIR-RED}{NIR+RED}$	Rouse et al. 1974

diversity measured in the sub-plots and the spectral & texture properties obtained from the satellite images. The Pearson correlation coefficient (PCC) was used to evaluate the association. PCC can be used when the data had a normal or near-normal distribution. Shapiro-Wilk method was used to test whether or not all variables had a normal distribution. When $P > 0,05$, the variable in question was considered to have a normal distribution (Kalaycı 2006; Kayitakire et al. 2006). The work flow used to identify the alpha diversity and associate it with the image properties is presented in Fig. 2.

Beta (β) Diversity

β diversity was calculated by using the rarefaction function. To this end, first of all rarefaction analysis was applied to obtain the values of the actual species diversity from the plots and the rarefaction curve was modeled depending on the presence and absence of the species in the plots. Taking into account of the

approach proposed by Rocchini et al. (2009); the minimum accumulated number of species was taken as average alpha ($\bar{\alpha}$) diversity while the maximum accumulated number of species was taken as gamma () diversity based on the rarefaction curve. The actual β diversity (β_{real}) was calculated as the difference between α and $\bar{\alpha}$. Then, the same procedure was applied to the brightness obtained from the satellite images and the spectral rarefaction curves were created.

In order to estimate the β diversity with the help of the image *brightness* values, the relationship between the species rarefaction values and the spectral rarefaction values was tested through employing the multiple regression models. The stepwise selection procedure was applied to develop a model. With the help of the most compatible models, the species rarefaction curves were remodeled, based on which the estimated β diversity (β_{est}) values were found. B_{est} values and β_{real} values were compared on the basis of three satellite images. There is a need for data from one band in order to model the rarefaction curves. Previous studies preferred PCA or NDVI (Rocchini et al., 2009, 2011). As we used satellite images with different number of bands in our study, it was decided to use NDVI image in order to ensure a standard between hem. Rarefaction functions were calculated based on 500 iterations through EstimateS (Version 9.1.0) software. The work flow, followed in the analysis of rarefaction is presented in Fig. 2.

Table 2 Spectral & textural properties used in the study

Image Properties	Equation*
Average brightness value	$\frac{1}{\#P_v} \sum_{(i,j) \in P} C_k(i, j)$
GLCM Contrast	$\sum_{i,j=0}^{N-1} P_{i,j}(i - j)^2$
GLCM Entropy	$\sum_{i,j=0}^{N-1} P_{i,j}(-\ln P_{i,j})$
GLCM Correlation	$\sum_{i,j=0}^{N-1} P_{i,j} \left[\frac{(i-\mu_i)(j-\mu_j)}{\sqrt{(\sigma_i^2)(\sigma_j^2)}} \right]$

*Parameters (Definiens 2006)

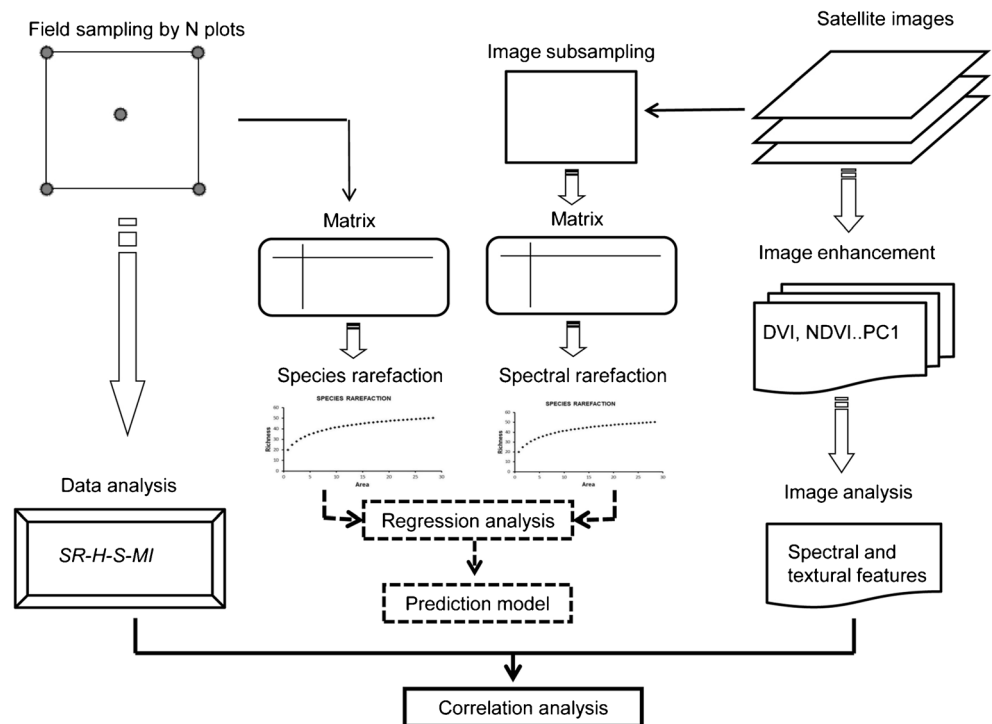
i is the row number; j is the column number; P_v is the cluster of pixels of the image object; $\#P_v$ is the total number of current pixels in P_v ; (i,j) is the coordinates of pixels; $c_k(i,j)$ is the pixel value; $P_{i,j}$ is the normalized value in the cell i, j; N is the number of columns and rows; μ_i and μ_j represent the average of the row i and column j; σ_i and σ_j represent the standard deviation of the row i and column j.

Table 3 Indicators of alpha diversity used in the study

Diversity Indicators	Equation
Species Richness	$SR = N$
Shannon-Wiener Diversity Index	$H' = -\sum p_i \ln(p_i)$
Simpson's Diversity Index	$S = 1 - \sum n_i(n_i - 1)/N(N - 1)$
Species Mingling Index	$MI_i = \frac{1}{4} \sum_{j=1}^4 V_{ij}$

n_i is the number of individuals in species i, N: is the total number of individuals in the community, P_i = is the proportion of each species in the sample, $\ln P_i$ = natural logarithm of this proportion, $V_i - 1$ if reference tree i and neighbor j are of different tree species; 0 otherwise,

Fig. 2 Flow chart of the methodology applied



Results

Relationships Between Alpha Diversity and Satellite-Based Variables

The relationship between alpha diversity and the spectral & texture properties of the image was observed to be linear or near-linear; therefore, the relationship between the image properties and the indicators of α diversity was evaluated through PCC. Statistically significant relationships were found between diversity indicators calculated on the basis of terrestrial measures and the spectral & texture properties obtained from the satellite images. To sum up, the *Brightness* derived from the red band of RapidEye image had a statistically significant relationship with *S* (Table 4). The *Brightness* derived from the near infrared band showed a significant relationship with *S* and *MI*. Moreover, the *Brightness* derived from NDVI and ARVI were associated with all the diversity indicators. ARVI *Brightness* had the strongest relationship with *S* and *H'* ($r = 0.80$ and 0.75 $p < 0.01$). Apart from the spectral values, the texture properties obtained from RapidEye image were observed to have significant relationships with the diversity indicators. Among the texture properties, *GLCM Contrast* had a significant relationship with *SR* in the red band and vegetation indexes. In contrast, the relationship between the *GLCM Contrast* and *MI*, *S* and *H'* was, in general, weak on all bands. *GLCM Correlation* had a significant relationship, in general, with *SR*; whereas the relationship between *MI*, *S* and *H'* and *GLCM Correlation* was observed to be weak on all bands. Besides, *GLCM Entropy* also had a statistically

significant relationship with *SR* on the red band. Among the *texture* properties, the strongest relationship was observed to be between the *GLCM Contrast* derived from IPVI and *SR* ($r = 0.57$, $p < 0.01$).

The strongest relationship between the image properties derived from ASTER image and indicators of α diversity was observed between the *Brightness* derived from NDVI and *S* ($r = 0.55$, $p < 0.01$) (Table 5). It was understood that the *Brightness* derived from the vegetation indexes other than NDVI had, in general, significant relationships with *S*, *H'* and *MI*. Furthermore, significant relationships were found between the *Brightness* and *S* in the red band, and between the *Brightness* and *S* and *MI* on the near infrared band. The strongest relationship between the texture properties and the diversity indicators was found between the *GLCM Contrast* derived from the red band and *SR* ($r = 0.56$, $p < 0.01$). Furthermore, the *GLCM Contrast* on green and red bands highlight a significant relationships with *H'*, *S*, *MI* and *SR*. The original bands of ASTER image and *GLCM Entropy* obtained from the vegetation indexes were, in general, associated with all diversity indicators. The relationship between the *GLCM Entropy* derived from DVI and *SR* was calculated as $r = 0.56$ ($p < 0.01$). As another texture property, *GLCM Correlation* in all vegetation indexes had, in general, significant relationships with all diversity indicators.

The *Brightness* derived from the coastal and red bands of Landsat-8 with a spatial resolution of 30×30 m had significant relationships with *SR* and *S* (Table 6). The *Brightness* derived from the vegetation indexes, however, were observed to have significant relationships with *S* and *MI*. Only the

Table 4 Pearson correlation coefficients between spectral & texture features and indicators of α diversity (RapidEye)

		Band 1	Band 2	Band 3	Band 4	Band5	ARVI	DVI	IPVI	NDVI
<i>Brightness</i>	<i>SR</i>	0346*	0272	-0150	0,399*	0,288	0,669*	-0,004	-0,098	0,333
	<i>MI</i>	-0,100	-0,187	-0,349*	0,013	0,469**	0,674**	0,296	0,227	0,511**
	<i>H'</i>	0,006	-0,116	-0,336*	0,061	0,381*	0,744**	0,163	0,089	0,476**
	<i>S</i>	-0,191	-0,288	-0,503**	-0,054	0,503**	0,798**	0,336	0,274	0,625**
<i>GLCM Contrast</i>	<i>SR</i>	-0,352*	-0,103	-0,422*	-0,107	-0,209	-0,43**	-0,392*	-0,568**	-0,494**
	<i>MI</i>	0,009	0,165	0,004	0,161	0,119	-0,191	-0,140	-0,276	-0,216
	<i>H'</i>	0,005	0,184	-0,071	0,148	0,027	-0,210	-0,184	-0,362*	-0,260
	<i>S</i>	0,130	0,215	0,032	0,172	0,026	-0,177	-0,208	-0,336*	-0,202
<i>GLCM Entropy</i>	<i>SR</i>	-0,316	-0,303	-0,424*	-0,210	0,099	-0,326	-0,053	-0,229	-0,370*
	<i>MI</i>	-0,095	-0,003	-0,095	-0,029	0,363*	-0,094	0,227	-0,035	-0,113
	<i>H'</i>	-0,063	-0,007	-0,111	0,008	0,362*	-0,072	0,262	-0,008	-0,108
	<i>S</i>	0,011	0,059	-0,024	0,046	0,382*	-0,032	0,255	0,016	-0,051
<i>GLCM Correlation</i>	<i>SR</i>	0,312	0,052	0,313	0,122	0,285	0,422**	0,445**	0,553**	0,495**
	<i>MI</i>	0,028	-0,100	0,055	-0,106	-0,010	0,175	0,206	0,253	0,208
	<i>H'</i>	0,071	-0,094	0,135	-0,084	0,064	0,231	0,276	0,357*	0,290
	<i>S</i>	-0,025	-0,078	0,066	-0,069	0,073	0,216	0,305	0,331	0,242

*Correlation is significant at the 0,05 level (2-tailed)

**Correlation is significant at the 0,01 level (2-tailed)

GLCM Correlation out of the texture properties that were derived from the red band had a significant relationship with *SR*. Apart from this, the texture properties derived from the original bands of Landsat-8 satellite image and vegetation indexes had very weak relationships with *H'*, *S*, *MI* and *SR*. The strongest relation between the image properties of

Landsat-8 and indicators of α diversity was found between the *Brightness* derived from NDVI and *S* ($r = 0.50, p < 0.01$).

Modeling Species Rarefaction Curves based on Spectral Rarefaction Curves

The species and spectral rarefaction curves modeled as a result of the rarefaction analysis in the study are presented in

Table 5 Pearson correlation coefficients between spectral & texture features and indicators of α diversity (ASTER)

		Band 1	Band 2	Band 3	DVI	IPVI	NDVI
<i>Brightness</i>	<i>SR</i>	0,169	0,312	0,176	0,155	0,179	0,179
	<i>MI</i>	-0,247	-0,339*	0,407*	0,432**	0,468**	0,468**
	<i>H'</i>	-0,226	-0,298	0,302	0,337*	0,384*	0,385*
	<i>S</i>	-0,363*	-0,470**	0,434**	0,499**	0,549**	0,549**
<i>GLCM Contrast</i>	<i>SR</i>	-0,265	-0,562**	-0,099	-0,292	-0,347*	-0,330
	<i>MI</i>	-0,421*	-0,288	-0,007	-0,214	-0,334	-0,306
	<i>H'</i>	-0,406*	-0,417*	-0,032	-0,242	-0,353*	-0,328
	<i>S</i>	-0,418*	-0,274	-0,041	-0,229	-0,343*	-0,316
<i>GLCM Entropy</i>	<i>SR</i>	0,140	0,406*	0,442**	0,655**	0,560**	0,538**
	<i>MI</i>	-0,059	-0,022	0,028	0,326	0,275	0,327
	<i>H'</i>	0,001	0,082	0,149	0,430**	0,437**	0,473**
	<i>S</i>	-0,005	-0,106	0,085	0,332	0,334	0,379*
<i>GLCM Correlation</i>	<i>SR</i>	0,330	0,378*	0,146	0,407*	0,441**	0,421*
	<i>MI</i>	0,221	0,347*	0,033	0,275	0,330	0,382*
	<i>H'</i>	0,295	0,392*	0,053	0,355*	0,402*	0,443**
	<i>S</i>	0,267	0,328	0,021	0,318	0,369*	0,414*

*Correlation is significant at the 0,05 level (2-tailed)

**Correlation is significant at the 0,01 level (2-tailed)

Table 6 Pearson correlation coefficients between spectral & texture features and indicators of α diversity (Landsat-8)

		Band 1	Band 2	Band 3	Band 4	Band5	Band6	ARVI	DVI	IPVI	NDVI
Brightness	SR	0,402*	0,312	0,176	0,074	0,067	0,192	0,095	0,051	0,116	0,116
	MI	-0,178	-0,161	-0,256	-0,330	-0,343*	-0,059	0,408*	0,371*	0,448**	0,448**
	H'	-0,177	-0,130	-0,253	-0,314	0,211	-0,110	0,295	0,246	0,349*	0,349*
	S	-0,217	-0,268	-0,366*	-0,450**	0,343*	-0,034	0,435**	0,391*	0,495**	0,495**
GLCM Contrast	SR	0,158	-0,151	-0,085	-0,120	0,241	-0,040	0,113	-0,043	-0,083	-0,083
	MI	0,117	-0,125	-0,027	-0,141	0,216	0,152	0,155	-0,063	-0,106	-0,106
	H'	0,077	-0,225	-0,121	-0,189	0,147	0,128	0,042	-0,146	-0,167	-0,167
	S	0,168	-0,229	-0,077	-0,182	0,182	0,134	0,071	-0,178	-0,222	-0,222
GLCM Entropy	SR	0,158	0,203	0,168	0,204	0,034	0,142	0,135	0,012	0,251	0,251
	MI	0,046	-0,068	-0,170	-0,029	0,075	-0,307	0,252	-0,165	0,129	0,129
	H'	0,117	0,034	-0,067	0,117	0,059	-0,280	0,238	-0,114	0,140	0,140
	S	-0,013	0,001	-0,153	-0,012	-0,006	-0,297	0,182	-0,113	0,165	0,165
GLCM Correlation	SR	-0,103	0,007	0,158	0,408*	-0,040	-0,197	-0,167	0,081	0,100	0,100
	MI	-0,125	0,048	0,109	0,071	-0,090	-0,249	-0,193	0,072	-0,034	-0,034
	H'	-0,152	0,101	0,146	0,223	0,005	-0,252	-0,146	0,085	0,011	0,011
	S	-0,152	0,085	0,162	0,127	-0,022	-0,254	-0,162	0,070	-0,060	-0,060

*Correlation is significant at the 0,05 level (2-tailed)

**Correlation is significant at the 0,01 level (2-tailed)

Fig. 4. According to the species rarefaction curve; the average number of species of the sampling units ($\bar{\alpha}_{real}$) was 20, while the actual total number of species in the sampling units (γ_{real}) was 50 and the diversity between the sampling units (β_{real}) was 30 (Fig. 3). The species rarefaction curve rose quickly until the seventh sampling unit, after which the rising trend of the curve slowed down. This trend of the rarefaction curve shows that there is a low species difference between the sampling units. The trends in the spectral rarefaction curves were similar to those of the species rarefaction curve. It can be concluded based on spectral rarefaction curves that the spectral difference between the image windows corresponding to the sampling units was low on each of the three satellite images.

According to the results of the multiple regression analyses between the species rarefaction values and spectral rarefaction values, very strong and positive relationships

were found between the species and spectral rarefaction values (Fig. 4). The relationships between the spectral rarefaction values derived from RapidEye NDVI, ASTER NDVI and Landsat-8 NDVI images and species rarefaction values (respectively $R^2 = 0.99, 0.99, 0.98$) were found to be similar. The species rarefaction curves that were remodeled according to those relationships are presented in Figure 5. According to these curves; $\bar{\alpha}_{est}$ was estimated to be 20, γ_{est} to be 47 and β_{est} to be 27 based on the spectral properties of Landsat-8 NDVI image. $\bar{\alpha}_{est}$, γ_{est} and β_{est} were estimated to be 20, 50, and 30 respectively, according to the ASTER NDVI image and to be 19, 50 and 31, respectively according to the RapidEye NDVI image. According to these findings; β diversity between the sampling units could be estimated accurately by using the brightness in the satellite images.

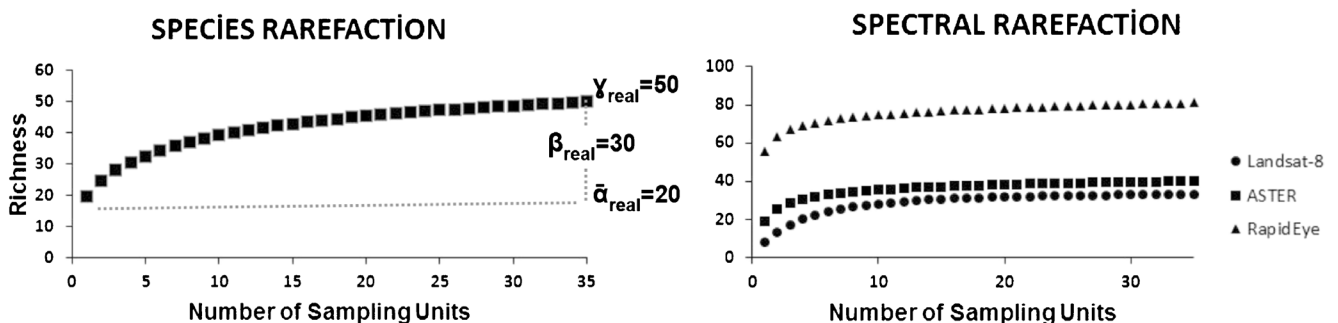


Fig. 3 Species and spectral rarefaction curves

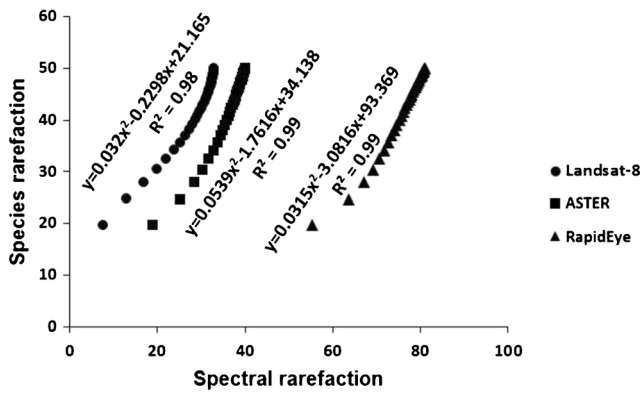


Fig. 4 Modeling of the relationship between the species and spectral rarefaction values

Discussion

The findings of the study demonstrate that satellite images can be useful tools to evaluate the α diversity in the urban forest remnants. The results of the correlation analysis revealed that there were statistically significant relationships between the spectral & texture properties of the image and α diversity. The strongest relationship between the indicators of α diversity and spectral values was found between the *Brightness* derived from ARVI of RapidEye satellite image and *S*. The *Brightness* derived from ARVI and other indicators of α diversity that were *SR*, *H'* and *MI* also had strong relationships. On ASTER satellite image, the strong relationship between the image properties and indicators of α diversity was observed to be between the *Brightness* derived from NDVI and *S*. The coastal, red bands of Landsat-8 satellite image as well as some vegetation indexes

were found to have statistically significant relationships with the diversity indicators. However, the level of such relationships was rather weaker compared to the other two satellite images because of mixed pixels. In the light of these findings, it can be suggested that it could be possible to evaluate the species diversity of a specific area by using the spectral values of an image.

These findings are also consistent with the results of similar studies that were conducted previously. For instance; Rocchini et al. (2004) verified the “spectral variation hypothesis” by using QuickBird image, according to which the areas with the highest spectral variation are expected to have the highest species richness. In another study conducted by Rocchini et al. (2007), the effect of the bands in evaluating the local species richness using the QuickBird satellite image was tested, while it concluded that near infrared band could be used for such evaluation. Bawa et al. (2002) studied the potential use of satellite images in order to identify the areas that had low and high species richness in tropical forests. This study in which NDVI derived from IRS 1C LISS III was used revealed that there was a high and positive relationship between NDVI and species richness ($R^2 = 0.63$ in broad-leaved forests, 0.42 in macquis shrub lands, and 0.66 in all vegetation types). Levin et al. (2007) conducted a study in which they tested the relationship between the NDVI images derived from Landsat, Aster and QuickBird satellite images and plant species richness. They concluded that there was a positively significant relationship between all of the NDVI images and plant richness (with R^2 as high as 0.87 between NDVI and total plant richness and 0.89 for annual plant richness).

The results obtained demonstrate that the texture properties of an image can be used to evaluate α diversity in

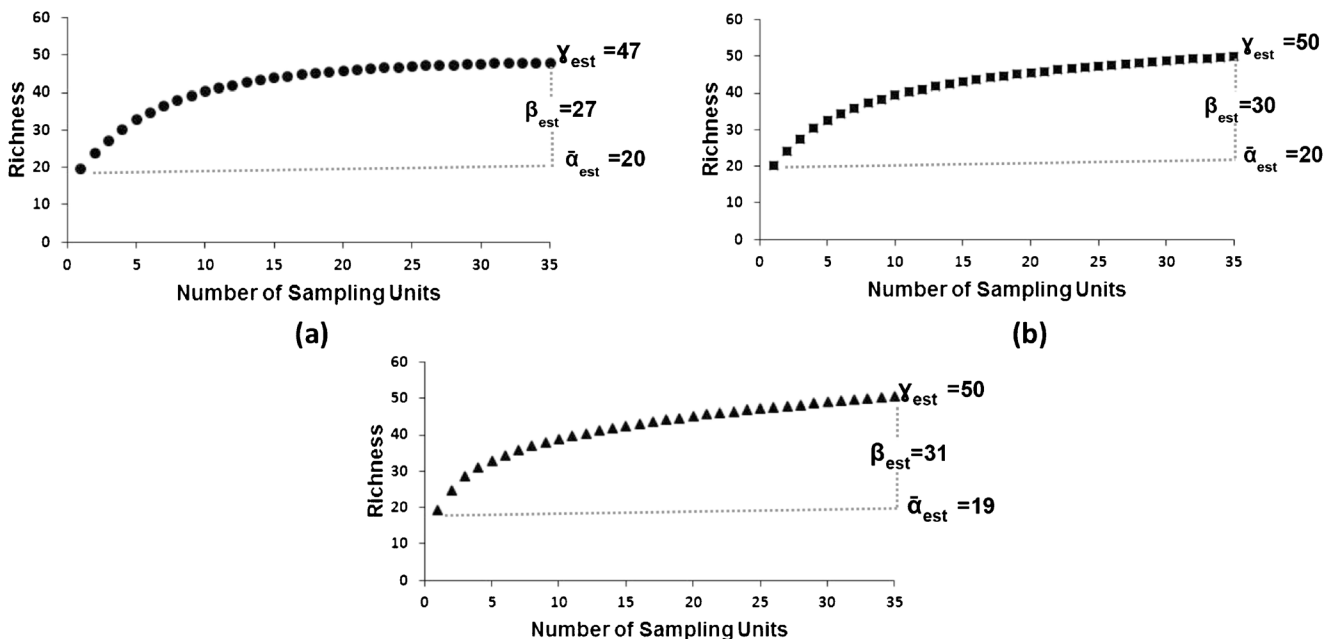


Fig. 5 Estimation of the species rarefaction curves (a-Landsat-8 b-ASTER c-RapidEye) and β diversity based on the spectral rarefaction curves

addition to the *Brightness*. *GLCM Contrast*, *GLCM Entropy* and *GLCM Correlation* were observed to have statistically significant relationships with *SR* on RapidEye image. The strongest relationship was found between the *GLCM Contrast* values and *SR*. On ASTER image; some significant relationships were observed between the texture properties and diversity indicators. The strongest relationship was found to be between the *GLCM Contrast* and *GLCM Entropy* values and *SR*. On Landsat-8 image, however, only the *GLCM Correlation* and *SR* had a significant relationship. To the best of our knowledge, there is no other study that evaluated the relationship between the texture properties of the satellite image and species diversity, the findings of this study could not be compared directly with the relevant studies in the literature. However, it was reported that some texture properties obtained from satellite images could be used both at stand level (Ozdemir and Karnieli 2011) and landscape level (Ozdemir et al. 2012) to determine the heterogeneity of the forest structure. Moreover, in the study conducted by Ozkan (2014) it concluded that the texture properties of the image were high due to the increased heterogeneity in the areas with greater species diversity. Therefore, it can be suggested that the findings of this study are partially consistent with the relevant literature.

The results of the study showed that spectral rarefaction curves could be used as an important method to estimate β diversity in urban forest remnants. According to the multiple regression analysis, very high positive relationships were found between the species and spectral rarefaction values. Based on the species rarefaction curves that were remodeled according to those relationships, β diversity could be estimated with high precision. These results are, in general, consistent with the findings of the similar studies performed previously. In a study conducted by Rocchini et al. (2009) who used Landsat ETM+ satellite image, the species diversity in different regions was compared based on the spectral rarefaction curves and they emphasized that it was a strong tool to identify the differences in biological diversity between the regions. In another study conducted by Rocchini et al. (2011) using Landsat ETRM+ satellite image, the relationship between the species rarefaction and spectral rarefaction was evaluated on the basis of the growth rates in the rarefaction curves. They found high and positive relationships between the species rarefaction and spectral rarefaction ($r = 0.88; 0.95$ $p < 0.001$). Based on those results, they concluded that spectral rarefaction curves could be used as a quick method to estimate the differences in vegetation diversity at regional scale.

In our study, three satellite images with different spatial resolution were tested in the evaluation of woody species diversity in urban forest remnants. For α diversity, RapidEye and ASTER satellite images with a spatial resolution of 5 m

and 15 m had similar results, while the results of Landsat-8 satellite image with a spatial resolution of 30 m were lower than the others. For the estimation of β diversity, none of the satellite images were superior to another. Therefore, low-cost medium resolution satellite images (Landsat) can be used to estimate β diversity in urban forest remnants based on rarefaction.

This study demonstrated that satellite images could be used to evaluate the woody species diversity in urban forest remnants and its temporal variations. The species diversity could not be precisely identified on the satellite images due to the inability to evaluate the species in the substrata because of crown closure or due to specific challenges such as complicated pixels (Rocchini et al. 2011). However, it would be possible to identify the areas that are rich or poor in species diversity. Therefore, it could be possible to decide where to concentrate the sampling to collect the data needed for future planning of these areas. This can result in more sound data regarding the species diversity in a specific area. Moreover, the temporal variation in the species diversity can be quickly and practically evaluated through the analysis of satellite images recorded on different dates. In this way, the hot points where the protection strategies can be focused could be identified easily during planning. Hence, it would be useful to continue evaluating the possibilities of using next-generation remotely sensed data with different spatial and spectral resolution for this purpose.

Conclusions

The results revealed that the woody species diversity at α level and the spectral & texture properties. The strongest relationship was found between the *Brightness* derived from Atmospherically Resistant Vegetation Index (ARVI) of RapidEye image and *Simpson's Diversity Index (S)*. A very high correlation was found between the spectral rarefaction values and species rarefaction values. It was revealed that β diversity could be estimated with high precision through employing species rarefaction curves modeled on the basis of the spectral rarefaction curves. The woody species diversity in urban forest remnants can be evaluated at α and β levels by employing the spectral & texture properties derived from the satellite images. Based on findings, it is concluded that the satellite images can be used to obtain reliable data more quickly as compared to other field survey methods due to having a significant potential. However, the satellite image with a resolution of 5 m would be more appropriate to estimate the woody species diversity of urban forest remnants. Hence, we recommended that the satellite image with a resolution of 5 m would be used in future for planning and conservation of urban forest remnants in a sustainable manner.

Acknowledgments This study was supported by the Scientific and Technological Research Council of Turkey (TÜBİTAK) under the project no 114O015. We would like to thank first and foremost TÜBİTAK for its support. Furthermore, we would like to thank Istanbul University, Faculty of Forestry for facilitating our study. We would like to thank Istanbul Metropolitan Municipality for allowing us to perform our study in the urban forest remnants that are under its ownership. Lastly, we thank to Dr. Rajpar Muhammad Nawaz for English editing of our paper.

References

- Adam, E. M., Mutanga, O., Rugege, D., & Ismail, R. (2012). Discriminating the Papyrus Vegetation (*Cyperus papyrus* L.) and its co-Existent Species Using Random Forest and Hyperspectral Data Resampled to HYMAP. *International Journal of Remote Sensing*, 33(2), 552–569.
- Alvey, A. A. (2006). Promoting and Preserving Biodiversity in the Urban Forest. *Urban Forestry & Urban Greening*, 5(4), 195–201.
- Ardila, J. P., Bijker, W., Tolpekin, V. A., & Stein, A. (2012). Context-Sensitive Extraction of Tree Crown Objects in Urban Areas Using VHR Satellite Images. *International Journal of Applied Earth Observation and Geoinformation*, 15, 57–69.
- Asan, U., Özkan, U. Y., Zengin, H., & Sağlam, S. (2007). Principals of Application of Ecosystem Based Functional Planning Approach in City Groves. In *Proceedings of Bottlenecks, Solutions, and Priorities in the Context of Functions of Forest Resources International Symposium*, Istanbul, pp. 227–242.
- Bagnall, R. G. (1979). A Study of Human Impact on a Urban Forest Remnant: Redwood Bush, Tawa, near Wellington, New Zealand. *New Zealand Journal of Botany*, 17(2), 117–126.
- Battles, J. J., Shlisky, A. J., & Barrett, R. H. (2001). The Effects of Forest Management on Plant Species Diversity in a Sierran Conifer Forest. *Forest Ecology and Management*, 146(1), 211–222.
- Bawa, K., Rose, J., Ganeshiah, K. N., Barve, N., Kiran, M. C., & Umashaanker, R. (2002). Assessing Biodiversity from Space: An Example from the Western Ghats, India. *Conservation Ecology*, 6(2), 7.
- Cayuela, L., Benayas, J. M., Justel, A., & Salas-Rey, J. (2006). Modelling Tree Diversity in a Highly Fragmented Tropical Montane Landscape. *Global Ecology and Biogeography*, 15, 602–613.
- Crippen R. E. (1990). Calculating the vegetation index faster. *Remote Sensing of Environment*, 00334(1), 71–73.
- Definiens, A. G. (2006). *Definiens professional 5 reference book*. Munich: Definiens AG.
- Dian, Y., Li, Z., & Pang, Y. (2015). Spectral and Texture Features Combined for Forest Tree species Classification with Airborne Hyperspectral Imagery. *Journal of the Indian Society of Remote Sensing*, 43(1), 101–107.
- Fairbanks, D. H. K., & McGwire, K. C. (2004). Patterns of Floristic Richness in Vegetation Communities of California: Regional Scale Analysis with Multi-Temporal NDVI. *Global Ecology and Biogeography*, 13, 221–235.
- Forman, R. T. T. (2014). *Urban ecology: Science of cities*. Cambridge: Cambridge University Press.
- Gadow, K. V., & Hui G. (2002). Characterising forest spatial structure and diversity. In *Proceedings of in Sustainable Forestry in Temperate Regions. Proceedings of the SUFOR International Workshop*, Lund University, pp. 20–30.
- Gillespie, T. W., Foody, G. M., Rocchini, D., Giorgi, A. P., & Saatchi, S. (2008). Measuring and Modelling Biodiversity from Space. *Progress in Physical Geography*, 32(2), 203–221.
- Harralick, R. M., Shanmugam, K., & Dinstein, I. (1973). Textural Features for Images Classification. *Systems, Man and Cybernetics, IEEE Transactions on*, 6, 610–621.
- Hung, M. C. (2002). Urban Land Cover Analysis from Satellite Images. *Pecora 15/Land Satellite Information IV/ISPRS Commission II/FIEOS 2002 Conference Proceedings*. <http://www.isprs.org/proceedings/XXXIV/part1/Paper/00099.pdf>. Accessed 15 January 2015.
- Jensen, J. R., & Lulla, K. (1996). *Introductory digital image processing, a remote sensing perspective*. New Jersey: Taylor & Francis.
- Kalayci, S. (2006). *SPSS uygulamalı Çok değişkenli istatistik teknikler*. Ankara: Asil yayın Dağıtım.
- Kark, S., & Dearborn, D. C. (2009). Motivations for Conserving Urban Biodiversity. *Conservation Biology*, 24(2), 432–440.
- Kaufman, Y. J., & Tanre, D. (1992). Atmospherically Resistant Vegetation Index (ARVI) for EOS-MODIS. *IEEE Transactions. Geoscience. Remote Sensing*, 30(2), 261–270.
- Kayitakire, F., Hamel, C., & Defourny, P. (2006). Retrieving Forest Structure Variables Based on Image Texture Analysis and IKONOS-2 Imagery. *Remote Sensing of Environment*, 102(3), 390–401.
- Kim, M., Warner, T. A., Madden, M., & Atkinson, D. S. (2011). Multi-Scale GEOBIA with Very High Spatial Resolution Digital Aerial Imagery: Scale, Texture and Image Objects. *International Journal of Remote Sensing*, 32(10), 2825–2850.
- Kong, F., Yin, H., & Nakagoshi, N. (2007). Using GIS and Landscape Metrics in the Hedonic Price Modeling of the Amenity Value of Urban Green Space: A Case Study in Jinan City, China. *Landscape Urban Planning*, 79, 240–252.
- Konijnendijk, C. C. (2005). *New perspectives for urban forests: Introducing wild woodlands*. In I. Kowaric, & S. Körner (Eds.), *Wild urban woodlands* (pp. 33–45). New York: Springer.
- Levin, N., Shmida, A., Levanoni, O., Tamari, H., & Kark, S. (2007). Predicting Mountain Plant Richness and Rarity from Space Using Satellite-Derived Vegetation Indices. *Diversity and Distributions*, 13(6), 692–703.
- Luoto, M., Toivonen, T., & Heikkinen, R. K. (2002). Prediction of Total and Rare Plant Species Richness in Agricultural Landscapes from Satellite Images and Topographic Data. *Landscape Ecology*, 17(3), 195–217.
- Mansfield, C., Pattanayak, S. K., McDow, W., McDonald, R., & Halpin, P. (2005). Shades of Green: Measuring the Value of Urban Forests in the Housing Market. *Journal of Forest Economics*, 11(3), 177–199.
- McKinney, M. L. (2002). Urbanization, Biodiversity, and Conservation. *Bioscience*, 52(10), 883–890.
- Moser, D., Zechmeister, H. G., Plutzer, C., Sauberer, N., Wrbka, T., & Grabherr, G. (2002). Landscape Patch Shape Complexity as an Effective Measure for Plant Species Richness in Rural Landscapes. *Landscape Ecology*, 17(7), 657–669.
- Mutowo, G., & Murwira, A. (2012). Relationship Between Remotely Sensed Variables and Tree Species Diversity in Savanna Woodlands of Southern Africa. *International Journal of Remote Sensing*, 33(20), 6378–6402.
- Nagendra, H. (2001). Using Remote Sensing to Assess Biodiversity. *International Journal of Remote Sensing*, 22(12), 2377–2400.
- Oldeland, J., Wesuls, D., Rocchini, D., Schmidt, M., & Jürgens, N. (2010). Does Using Species Abundance Data Improve Estimates of Species Diversity from Remotely Sensed Spectral Heterogeneity? *Ecological Indicators*, 10(2), 390–396.
- Ozdemir, İ., & Donoghue, D. N. M. (2013). Modelling Tree Size Diversity from Airborne Laser Scanning Using Canopy Height Models with Image Texture Measures. *Forest Ecology and Management*, 295, 28–37.
- Ozdemir, İ., & Karnieli, A. (2011). Predicting Forest Structural Parameters Using the Image Texture Derived from WorldView-2 Multispectral Imagery in a Dryland Forest, Israel. *International*

- Journal of Applied Earth Observation and Geoinformation*, 13(5), 701–710.
- Ozdemir, I., Norton, D. A., Ozkan, U. Y., Mert, A., & Senturk, O. (2008). Estimation of Tree Size Diversity Using Object Oriented Texture Analysis and Aster Imagery. *Sensors*, 8, 4709–4724.
- Ozdemir, I., Mert, A., & Senturk, O. (2012). Predicting Landscape Structural Metrics Using Aster Satellite Data. *Journal of Environmental Engineering and Landscape Management*, 20(2), 168–176.
- Ozkan, U. Y. (2014). Assessment of Visual Landscape Quality Using IKONOS Imagery. *Environmental Monitoring and Assessment*, 186(7), 4067–4080.
- Petr, P., Zdena, C., Antonin, P., Vojtech, J., Milan, C., & Lubomir, T. (2004). Trends in Species Diversity and Composition of Urban Vegetation over Three Decades. *Journal of Vegetation Science*, 15(6), 781–788.
- Rocchini, D. (2007). Effects of Spatial and Spectral Resolution in Estimating Ecosystem α -Diversity by Satellite Imagery. *Remote Sensing of Environment*, 111(4), 423–434.
- Rocchini, D., Chiarucci, A., & Loiselle, S. A. (2004). Testing the Spectral Variation Hypothesis by Using Satellite Multispectral Images. *Acta Oecologica*, 26(2), 117–120.
- Rocchini, D., Butini, S. A., & Chiarucci, A. (2005). Maximizing Plant Species Inventory Efficiency by Means of Remotely Sensed Spectral Distances. *Global Ecology and Biogeography*, 14(5), 431–437.
- Rocchini, D., Ricotta, C., & Chiarucci, A. (2007). Using Satellite Imagery to Assess Plant Species Richness: The Role of Multispectral System. *Applied Vegetation Science*, 10(3), 325–331.
- Rocchini, D., Ricotta, C., Chiarucci, A., De Dominicis, V., Cirillo, I., & Maccherini, S. (2009). Relating Spectral and Species Diversity Through Rarefaction Curves. *International Journal of Remote Sensing*, 30(10), 2705–2711.
- Rocchini, D., McGlenn, D., Ricotta, C., Neteler, M., & Wohlgemuth, T. (2011). Landscape Complexity and Spatial Scale Influence the Relationship Between Remotely Sensed Spectral Diversity and Survey-Based Plant Species Richness. *Journal of Vegetation Science*, 22(4), 688–698.
- Rouse, J. W., Haas, R. H., Jr., Schell, J. A., & Deering, D. W. (1974). Monitoring vegetation systems in the Great Plains with ERTS. In *Proceedings of Third ERTS-1 Symposium*, Washington DC, pp. 309–317.
- Sander, H., Polasky, S., & Haight, R. G. (2010). The Value of Urban Tree Cover: A Hedonic Property Price Model in Ramsey and Dakota Counties, Minnesota, USA. *Ecological Economics*, 69(8), 1646–1656.
- Shannon, C. E., & Weaver, W. (1949). *The mathematical theory of communication*. Urbana: University of Illinois Press.
- Simpson, E. H. (1949). Measurement of Diversity. *Nature*, 163, 688.
- Singh, J. S., Roy, P. S., Murthy, M. S. R., & Jha, C. S. (2010). Application of Landscape Ecology and Remote Sensing for Assessment, Monitoring and Conservation of Biodiversity. *Journal of the Indian Society of Remote Sensing*, 38(3), 365–385.
- Tucker, C. J. (1979). Red and Photographic Infrared Linear Combinations for Monitoring Vegetation. *Remote Sensing of Environment*, 8, 127–150.
- Tyrväinen, L., Pauleit, S., Seeland, K., & Vries, D. (2005). Benefits and uses of urban forests and tree. In C. Konijnendijk, K. Nilsson, T. Randrup, J. Schipperijn (Ed), *In urban forests and trees* (pp.81–114). New York: Springer.
- Varghese, A. O., Joshi, A. K., & Murthy, Y. K. (2010). Mapping of Realized and Fundamental Niches of Threatened Tree Species Using Geoinformatics: A Species Level Approach for Sustaining Biodiversity. *Journal of the Indian Society of Remote Sensing*, 38(3), 523–534.